Co-published by
Institute of Fluid-Flow Machinery
Polish Academy of Sciences
Committee on Thermodynamics and Combustion
Polish Academy of Sciences

Copyright©2026 by the Authors under licence CC BY-NC-ND 4.0

http://www.imp.gda.pl/archives-of-thermodynamics/

Experimental study of a reversible ventilation – heat pump system with a ceramic regenerator

Katarzyna Katana[a], Andrzej Grzebielec[a*], Adam Szelągowski[a], Maksymilian Kruk[a], Krzysztof Bruzi[b]

[a]Warsaw University of Technology, pl. Politechniki 1, 00-665 Warszawa, Poland
[b]Respireco sp. z o.o., Piaski 39, 63-300 Pleszew, Poland
*Corresponding author email: andrzej.grzebielec@pw.edu.pl

Received: 07.02.2026; revised: 23.05.2026; accepted: 29.05.2026

Abstract

Mechanical supply-exhaust ventilation systems are increasingly required in newly constructed residential buildings, yet their higher primary energy consumption remains a key challenge, particularly given the growing demands of energy efficiency and unchanged fresh air requirements. Existing solutions based on recuperators achieve heat recovery efficiencies of 40−70%, whereas regenerative systems can exceed 90%, but their performance under real operating conditions and integration with heat pump technology has not been sufficiently investigated. This study presents an experimental analysis of a compact ventilation unit, dedicated to classrooms, operating in reversible mode with a rotary regenerator and an integrated R290 (propane) air-to-air heat pump. Measurements were conducted across an outdoor temperature range from 0.6°C to 8.6°C. The regenerator-only mode achieved heat recovery efficiency exceeding 90% throughout the entire tested temperature range. When the R290 heat pump was activated to sustain operation during periods of lower outdoor temperatures without an auxiliary heat source, the system yielded COP values between 3.70 and 4.31, substantially higher than 2.0−2.5 values typically reported for conventional air-to-air heat pumps. These results demonstrate that the proposed integration of regenerative heat recovery with a dedicated R290 heat pump constitutes a technically viable and energy-efficient solution for both heating and ventilation needs.

Keywords: Ventilation; Ceramic regenerator; Heat recovery; Heat pump; Energy efficiency

Vol. 47(2026), No. 3, 15–24; doi: 10.24425/ather.2026.3650

Cite this manuscript as: Katana, K., Grzebielec, A., Szelągowski, A., Kruk, M., & Bruzi, K. (2026). Experimental study of a reversible ventilation – heat pump system with a ceramic regenerator. *Archives of Thermodynamics*, 47(3), 15−24.

1. Introduction

All buildings occupied by people must be equipped with a ventilation system, whose primary function is to supply fresh air and remove used one [1,2]. However, the requirements for ventilation performance vary depending on building function and occupancy characteristics [3]. Providing adequate indoor air quality (IAQ) represents one of the central challenges of contemporary building engineering. High occupant density combined with extended occupancy periods leads to rapid deterioration of indoor air quality, manifested primarily through elevated concentrations of CO_2 and particulate matter. Transitioning to mechanical supply-and-exhaust ventilation resolves the IAQ problem but introduces substantial heating energy penalties, which can reach 35−40 kWh/m² annually at the building level [4]. Among available heat recovery technologies, fixed bed regenerators (FBR) based on ceramic fill represent an alternative to the widely used rotary and crossflow plate heat exchangers [5,6]. The effectiveness of heat exchangers in heat recovery systems depends on airflow rate, temperature differences, and the moisture content of the air streams [7]. Figures 1 and 2 show the actual heat recovery effectiveness for crossflow and rotary heat exchangers, respectively, for the full ranges of available products [8].

Nomenclature

i – specific enthalpy, J/kg
$\dot{m}$ – air mass flow rate, kg/s
p – gauge pressure, bar
P – electrical power, W
q – air mass flow rate
Q – heat, J
$\dot{Q}$ – heat capacity, W
RH – relative humidity, %
t – time, s
W – electrical energy, J

Greek symbols

η – regenerator effectiveness,
θ – air temperature, °C
τ – time period, s

Subscripts and Superscripts

1,2,3,4 – process periods
11 – exhaust at inlet of regenerator
21 – supply at inlet of regenerator
22 – supply at outlet of regenerator
I – indoor air
II – condenser air side
III – outdoor air
IV – evaporator air side
cycle – amount for one cycle
el – electric
n – number of cycles

Abbreviations and Acronyms

IAQ – indoor air quality
COP – coefficient of performance
FBR – fixed bed regenerators
R290 – propane refrigerant

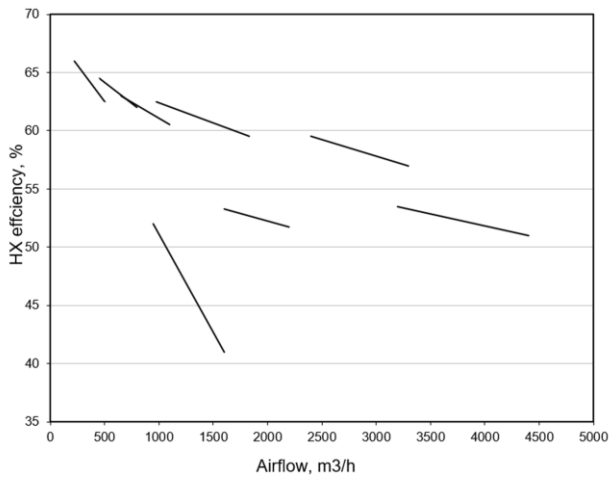


Fig. 1. Crossflow heat exchangers effectiveness (each line corresponds to one heat exchanger from the product range) [18].

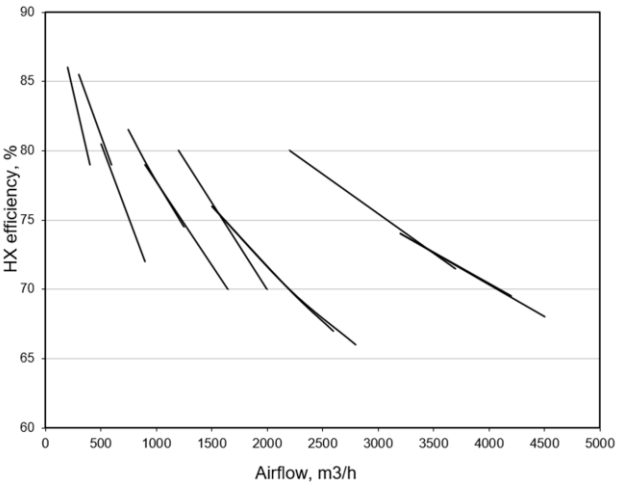


Fig. 2. Rotary heat exchangers effectiveness (each line corresponds to one heat exchanger from the product range) [18].

Each line corresponds to one heat exchanger from the product range. Results show that for rotary heat exchangers, effectiveness ranges from 40% to 66%. For each heat exchanger in the product range, effectiveness decreases when airflow increases (thus airflow speed). Similar results are obtained for rotary heat exchangers, but with higher effectiveness levels ranging from 65% to 86%.

Ceramic regenerators are characterised by a significantly greater heat transfer surface area per unit volume compared with recuperators, combined with the ability to recover both sensible and latent heat through adsorption and desorption of moisture on the porous ceramic surface [9]. The reversible operation of such devices, in which a single duct alternately serves as supply and exhaust, driven by a reversing fan, allows deployment without the need for separate supply and exhaust duct networks, making them particularly well-suited for retrofit applications in existing buildings. Commercial implementations of ceramic FBR ventilation units are currently offered by many manufacturers; however, systematic experimental characterisation of their performance under controlled conditions remains limited in the open literature.

A further improvement in energy efficiency can be achieved by integrating the ceramic regenerator with a heat pump. Exhaust air heat pumps (EAHP), which utilise the warm exhaust air stream as the heat source for the refrigeration circuit, represent an emerging class of ventilation and heating systems capable of simultaneously fulfilling the ventilation and space heating functions of a building [10]. The use of exhaust air at approximately 20°C as the heat source, rather than cold outdoor air, results in significantly more favourable evaporator operating conditions compared to conventional air-source heat pumps (ASHP), which translates directly into higher coefficients of performance [11]. The refrigerant R290 (propane) is an increasingly preferred working fluid for such applications due to its favourable thermodynamic properties and near-zero global warming potential (GWP) [12].

Despite the growing commercial interest in integrated ventilation – heat pump systems, published experimental data on systems combining a ceramic FBR regenerator with a heat pump

circuit are scarce. Niemierska and Jadwiszczak [5] investigated a ceramic FBR regenerator in a decentralised reversible ventilation system, reporting temperature effectiveness values above 80%, but without integration with a heat pump. Aktershev et al. [6] conducted a parametric numerical study of regenerative heat exchangers with periodic flow reversal. To the authors' knowledge, no experimental study has so far reported the combined performance of a ceramic fixed-bed regenerator integrated with an R290 air-to-air heat pump. The present paper addresses this gap. A laboratory test stand was constructed at the Institute of Heat Engineering, Warsaw University of Technology. The system was tested in both regenerator-only mode and heat pump mode. The primary objectives of this study were to develop a method for determining the temperature and total effectiveness of the ceramic FBR regenerator that accounts for the cyclic nature of its operation, and to experimentally characterise the heating capacity and coefficient of performance of the integrated system under varying outdoor conditions.

2. Materials and methods

Figure 3 shows the experimental laboratory setup and the locations of the temperature and relative humidity sensors. The purpose of the stand was to test the heat regeneration effectiveness of ceramic blocks and the operation of a heat pump with an incorporated regenerator. Propane (R290) was used as the working refrigerant. The total charge of propane was equal to 800 g. Although R290 is classified as a class A3 flammable refrigerant according to the PN-EN 378 standard, this charge quantity is permissible for rooms that meet the minimum space requirements or are equipped with a leak detection system that activates additional ventilation [13].

The stand is composed of:

- ventilation duct, inside of which is a reversible fan (which allows for the airflow to alternate between directions using a specialised guide vane);
- heat regenerator in a form of ceramic blocks;
- two heat exchangers associated with a heat pump;
- compressor with an inverter;
- 4-way valve;
- an expansion valve;
- refrigerant receiver;
- air filters at the inlet and outlet of the duct.

The test stand is equipped with an automation system that enables changing airflow direction, airflow rate, compressor rotational speed, heat exchangers operating mode (evaporator/condenser) and storing the refrigerant in a receiver.

Inside the device, there are two rows of ceramic blocks, 30 in total. The top row consists of 15 blocks with dimensions of 150 × 150 × 300 mm, whereas the bottom row has 15 shorter blocks measuring 150 × 150 × 72 mm. The masses are equal to 6.15 kg and 1.39 kg, respectively. The blocks are supported by thin-walled metal tubes. The total mass of the regenerator amounts to 113.1 kg, whereas the theoretical thermal capacity amounts to 99 528 J/K. The open flow area through each ceramic block is equal to approximately 0.01778 m². The physical layout of the ceramic blocks is presented in Fig. 4, while a photograph of the ceramic regenerator is shown in Fig. 5.

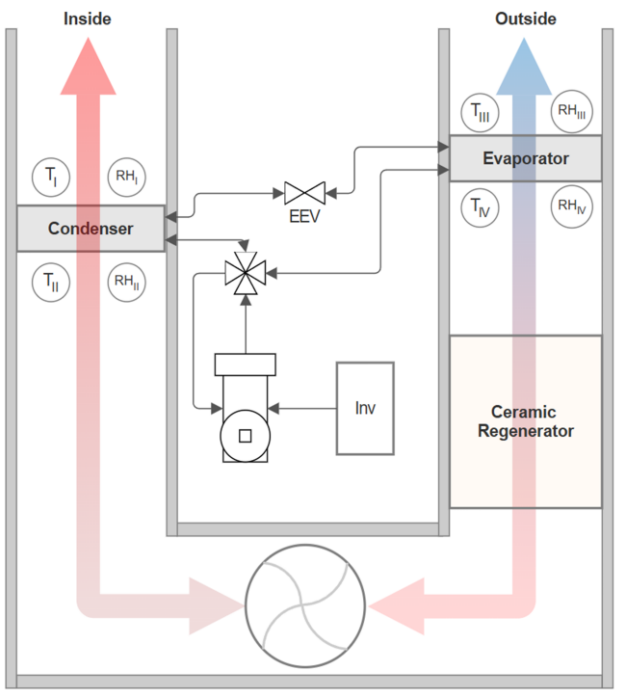


Fig. 3. Schematic diagram of the laboratory setup.

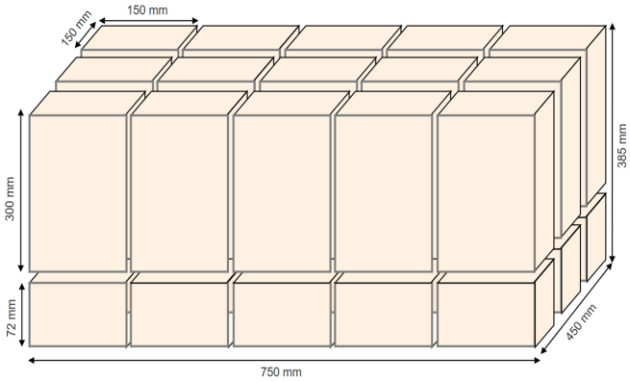


Fig. 4. Physical layout of ceramic blocks.



Fig. 5. Ceramic regenerator.

The device operates in two alternating modes. In an air supply phase, outdoor air flows through the ceramic regenerator, previously heated by the exhaust air removed from the room. As a result, the air supplied to the indoor space is preheated. During the air exhaust phase, indoor air is discharged to the outside while flowing through the said regenerator, which results in charging the heat storage. Additionally, incorporating a four-way valve allows the heat pump to operate in cooling mode during summer months.

NTC thermistors of accuracy class B were used for measuring temperature. In accordance with IEC 60539-1, the measurement tolerance of these sensors does not exceed ±0.425°C over the temperature range investigated in the device (from −10°C to 25°C) [14]. The relative humidity measurement accuracy is ±3% over the range of 20–80%, increasing linearly to ±4.5% for values outside this interval. An Iris-type damper (IRIS 250) was used to measure the airflow rate. The pressure difference was defined by two HK Instruments DPT250-R8 differential pressure transmitters, for which the measurement error is ±1%, corresponding to a maximum of ±8 Pa. The device also incorporated two Carel SPKT0041-DO pressure transducers on the refrigerant side, positioned at the discharge and suction ports of the compressor, corresponding to the condensation and evaporation pressures, respectively. Knowledge of the phase-transition pressures allows unambiguous determination of the condensation and evaporation temperatures. For this type of transducer, the measurement error does not exceed ±1%, which translates to a deviation of ±0.182 bar. To quantify the energy consumption of the control system, a Lumel N27P energy meter was employed, offering a measurement accuracy of 0.2% of the measuring range for active power, corresponding to approximately 2–3 W. The measurement instruments used in the experimental setup and their associated uncertainties are presented in Table 1.

Table 1. Measurement instruments and associated uncertainties used in the experimental setup.

Quantity	Instrument	Limit error	Standard uncertainty
Temperature	NTC class B	±0.425°C	0.245°C
Relative humidity	SHT20	±3% *RH* (20–80%), ±4.5% outside this range	1.732% RH
Airflow rate	IRIS250	±5%	2.887%
Air differential pressure	DPT250-R8	±1% of range	±8 Pa
Refrigerant pressure	Carel SPKT0041-DO	±1%	±0.182 bar
Electrical power	Lumel N27P	±0.2% of range	1.732 W

2.1. Ceramic regenerator effectiveness

In the first step, regenerator's effectiveness was tested for different temperature levels. Research was conducted in accordance with the norm: PN-EN 13141-8:2014-09 „Ventilation of buildings — Testing of performance of components/products for residential ventilation — Part 8: Testing of performance of ductless mechanical supply and exhaust units (including heat recovery) for mechanical ventilation systems" [10]. The device works periodically (supply/exhaust modes), and its cycle stages are shown in Fig. 6, where: τ_1 – time of air flow from the building to the outside, [s]; τ_2 – dwell time, [s]; τ_3 – time of air flow from the outside into the building, [s]; τ_4 – dwell time, [s]; $\dot{m}_{22}$ – mass flow rate of supply air at the outlet, [kg/s]; $\dot{m}_{11}$ – mass flow rate of exhaust air at the inlet, [kg/s].

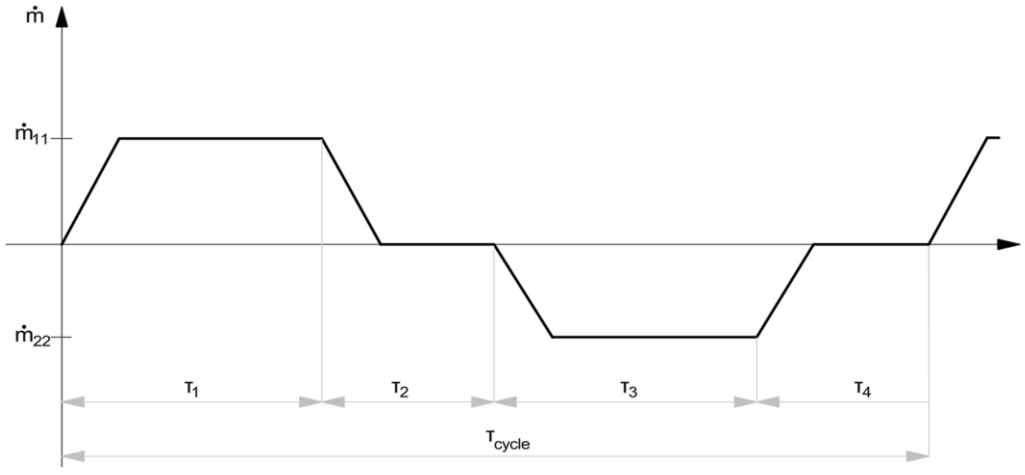


Fig. 6. Changes in the air mass flow rate as a function of time during one full cycle [19].

Times τ_1 and τ_3 correspond to the half time required for the fan guide vane to turn. The measured dwell time is equal to 4 s, therefore: τ_2 = 2.0 s and τ_4 = 2.0 s. This is the result of the device's design. The fan runs continuously, while the direction of airflow is changed by a guide vane; the fan is not turned off.

Therefore, the time to complete one full cycle is expressed as:

$$\tau_{cycle} = \tau_1 + \tau_2 + \tau_3 + \tau_4, [\text{s}]. \quad (1)$$

For this type of device, regenerator's effectiveness is defined by [15]:

$$\eta_\theta = \frac{\int(\theta_{22}-\theta_{21})\mathrm{d}t}{\int(\theta_{11}-\theta_{21})\mathrm{d}t} \cdot \frac{\dot{m}_{22}}{\dot{m}_{11}}, \quad (2)$$

where: θ_{22} – supply air temperature at the outlet of the heat recovery component, [°C]; θ_{21} – supply air temperature at the inlet of the heat recovery component, [°C]; θ_{11} – exhaust air temperature at the inlet of the heat recovery component, [°C].

Figure 7 presents regenerator's effectiveness results obtained during laboratory tests in accordance with Eq. (2) for the outside temperatures: −15°C, −7°C, +2°C, +7°C, and inside temperature equal to +20°C.

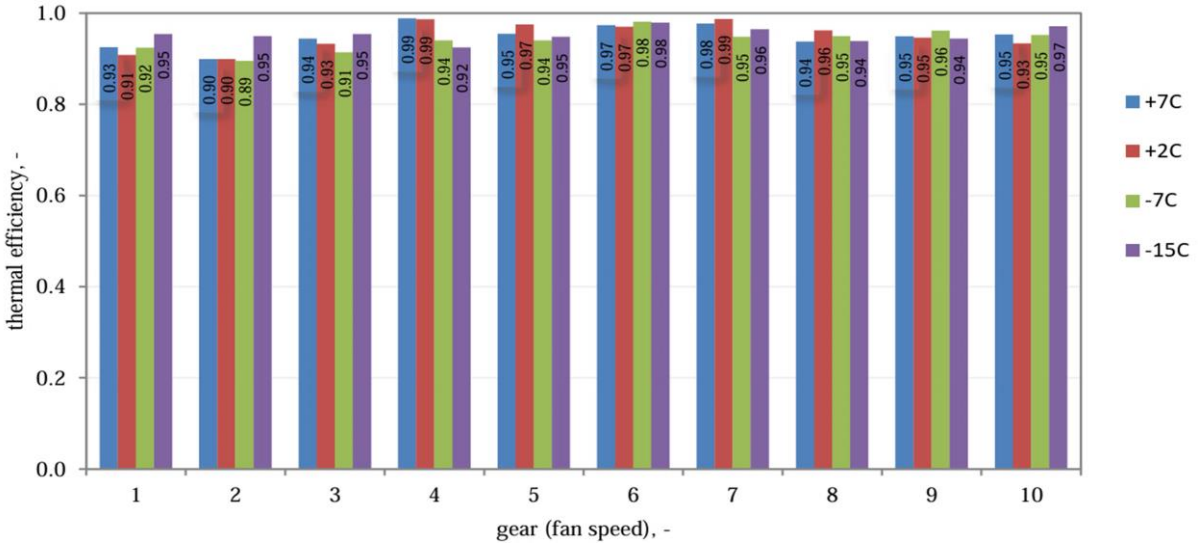


Fig. 7. Obtained ceramic regenerator's effectiveness.

In all analysed cases, the regenerator effectiveness exceeded 90%. The energy efficiency is influenced by the cycle duration and the length of the regenerator. In this article, only the results for the optimal cycle duration of 240 s and the optimal regenerator length are presented. Importantly, no water condensation occurred in the regenerator, which is a fundamental problem in the case of rotary and crossflow heat exchangers. In recuperators, electric preheaters are often used to preheat air to prevent condensation and water freezing. This solution significantly decreases heat recovery efficiency [16]. The absence of water vapour condensation in the ceramic regenerator can be attributed to two main factors. First, due to the short switching cycle in reversible operation mode, the ceramic mass is alternately heated and cooled at brief intervals, preventing its temperature from dropping to the dew point of the exhaust air. Second, the hygroscopic nature of the ceramic material allows moisture to be captured through adsorption rather than condensation, meaning that water vapour is retained within the material structure without forming a liquid phase.

2.2. Heat pump operation and performance

The heat supplied to the air stream was calculated from the difference in specific enthalpy between the supply and exhaust air. The specific enthalpy was calculated based on the temperature and relative humidity. The volumetric flow rate was measured using an ISA-standard nozzle equipped with pitot-tube measurements. The maximum supply air volumetric flow rate reached 1380 m³/h. The total heat supplied to the room during one cycle is given by:

$$Q_{cycle} = \int_{t=0}^{t=t_{half\ cycle}} \left[\dot{m}(t)\left(i_2(t) - i_3(t)\right)\right] dt,\ [\mathrm{J}], \quad (3)$$

where t = 0 [s] and $t_{half,cycle}$ [s] are, respectively, the time of beginning and ending of the half-cycle, $\dot{m}(t)$ [kg/s] is an air mass flow rate, $i_2(t)$ [kJ/kg] and $i_3(t)$ [kJ/kg] are, respectively, instantaneous specific enthalpies of the air supplied and removed.

The electrical energy supplied in one cycle consists of the energy used by the compressor, fan and automation system:

$$W_{cycle} = \int_{t=0}^{t=t_{cycle}} P_{el}\ (t)dt,\ [\mathrm{J}], \quad (4)$$

where t = 0 [s] and t_{cycle} [s] are, respectively, the beginning and ending times of the entire cycle, and $P_{el}(t)$ is the total electrical power supplied at a given moment.

This allows us to calculate the coefficient of performance (COP) during one cycle:

$$\mathrm{COP} = \frac{Q_{cycle}}{W_{cycle}}. \quad (5)$$

To determine the average heating capacity and electrical power, the total heat supplied and total electrical energy supplied were divided by the analysed time period:

$$\dot{Q}_{cycle} = \frac{Q_{cycle}}{\tau_1 - \tau_0},\ [\mathrm{W}], \quad (6)$$

$$P_{cycle} = \frac{W_{cycle}}{\tau_2 - \tau_0},\ [\mathrm{W}]. \quad (7)$$

3. Results and discussion

Studies of the vapour-compression heat pump with a regenerator were carried out for different outside temperatures in a range of 0.6°C to 8.6°C. The indoor air temperature was maintained approximately at 22°C. Each half-cycle of air supply and exhaust lasted 60 s, giving a full cycle duration of 120 s. Figure 8 shows the temperature changes over 30 full cycles (equivalent to 1 hour) at an outdoor temperature of 1.1°C. A close-up of tem-

perature changes during one cycle is shown in Fig. 9. The measured temperatures are: θ_I – indoor air temperature, [°C]; θ_{II} – condenser air-side temperature, [°C]; θ_{III} – outdoor air temperature, [°C]; θ_{IV} – evaporator air-side temperature, [°C].

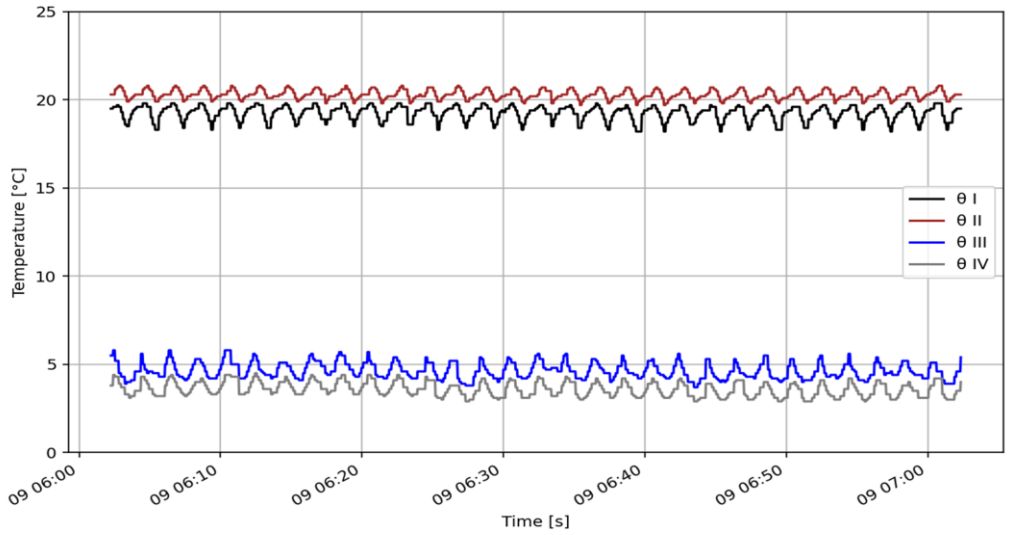


Fig. 8. Temperature changes during 30 full cycles.

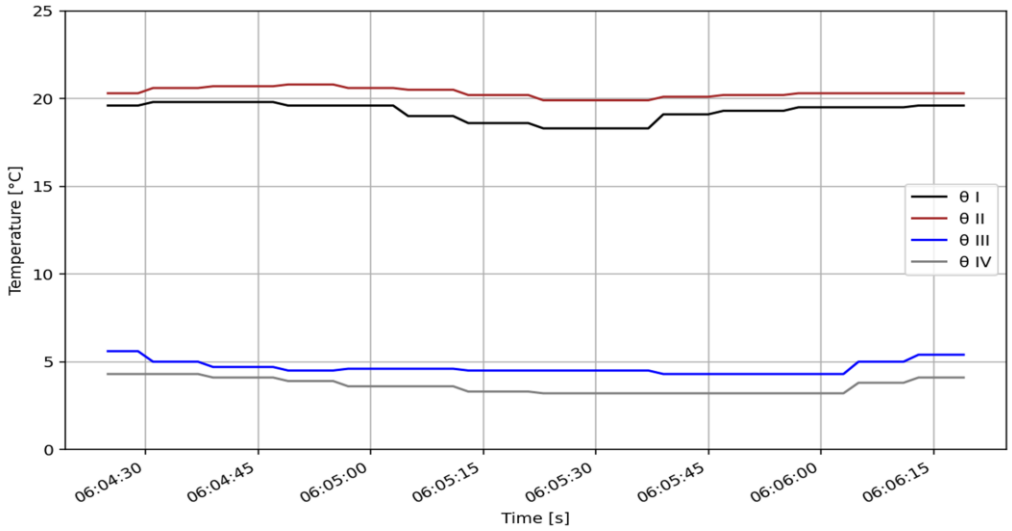


Fig. 9. Temperature changes during one full cycle.

Figure 10 presents changes in relative humidity during the same cycle as shown in Fig. 8. Measured relative humidities are: RH_I – indoor air relative humidity, [%]; RH_{II} – condenser air-side relative humidity, [%]; RH_{III} – outdoor air relative humidity, [%]; RH_{IV} – evaporator air-side relative humidity, [%]. The measuring points for temperature and relative humidity are shown in Fig. 3.

Figure 11 shows the changes in heating capacity and electrical power consumption during one full cycle for the outside temperature of 0.6°C. The electric power consumption varied only slightly, from 1150 W to 1220 W. The average heating capacity of this cycle was equal to 5306 W with a peak value exceeding 11 000 W, which is a result of accumulating heat in a ceramic regenerator. During the air exhaust phase, the heating capacity is equal to zero.

The experimental investigation of the device operating in heat pump mode was carried out under outdoor air temperature conditions ranging from 0.6°C to 8.6°C. The indoor temperature was equal to approximately 20°C, while the indoor relative humidity remained approximately 30% across all measurement series. The relatively low indoor relative humidity recorded throughout the experiments reflects the conditions of the laboratory facility in which the device was installed, rather than typical residential indoor climate conditions. The relative humidity of the outdoor air for the investigated measurement series as a function of outdoor temperature is presented in Fig. 12.

Refrigerant parameters remained stable across the tested outside temperature range. The system was operated to keep the discharge pressure at 15 bar. Refrigerant condensation and evaporation pressures are shown in Fig. 13. As the outdoor temperature increases, the evaporation pressure rises. This reduces the pressure difference between the suction and discharge sides of the compressor, resulting in lower power consumption and a higher COP.

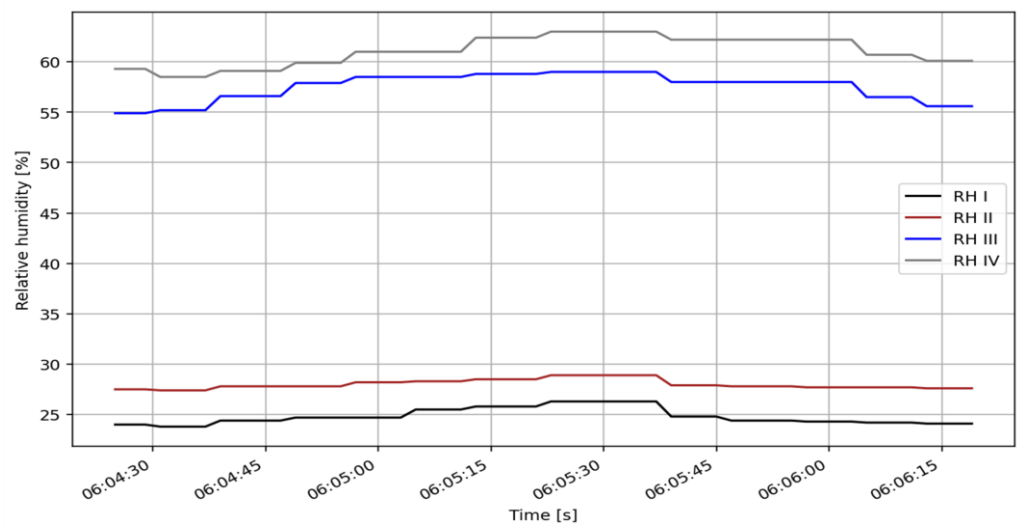


Fig. 10. Relative humidity changes during one full cycle.

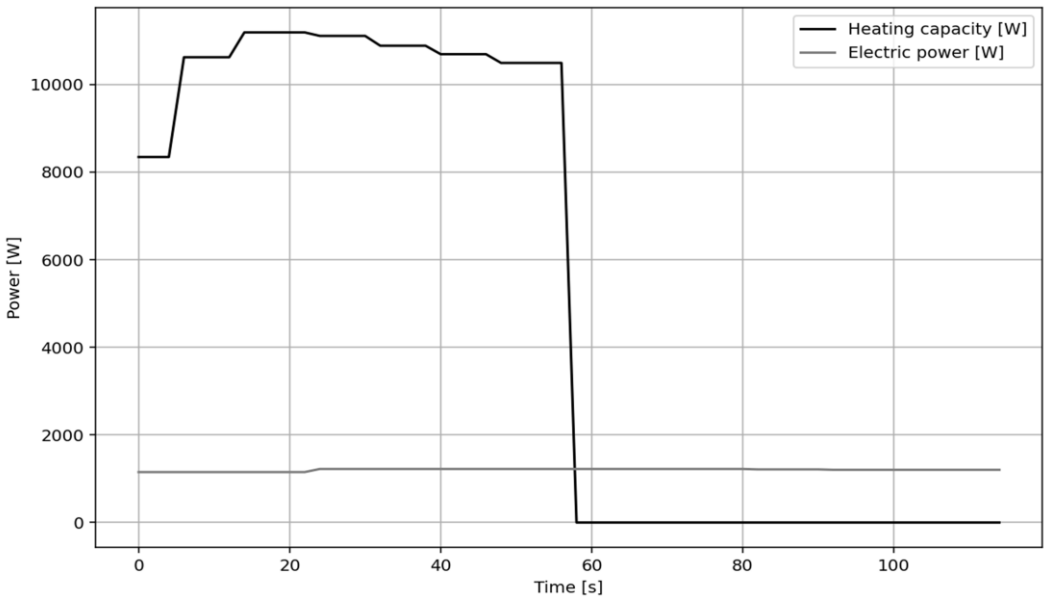


Fig. 11. Heating capacity and electrical power changes during one full cycle.

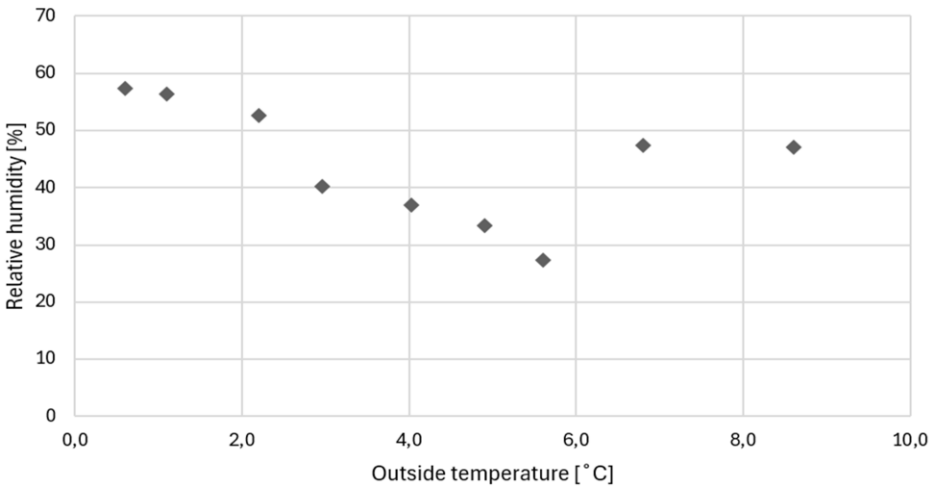


Fig. 12. Relative humidity vs. outside temperature.

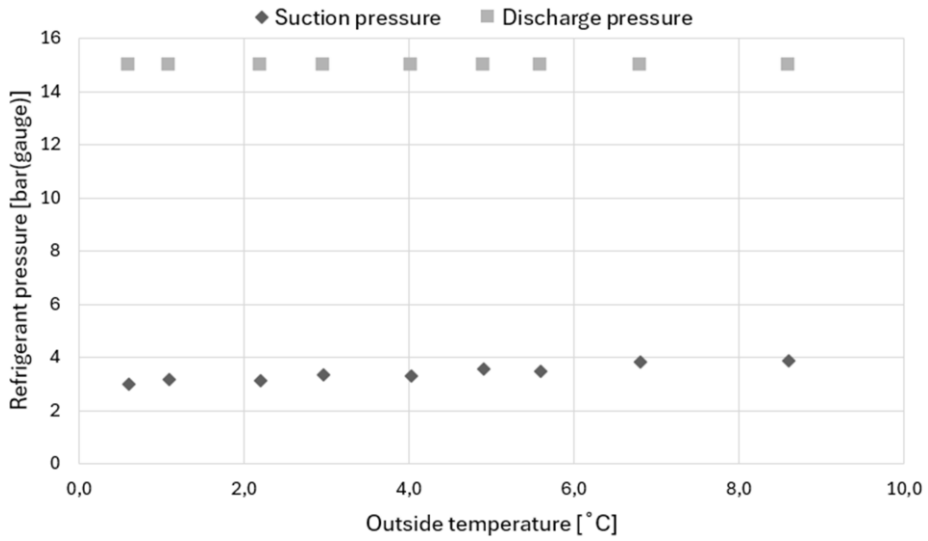


Fig. 13. Suction and discharge refrigerant gauge pressures vs. outside temperature.

The device's electrical power demand ranges from 1039 W to 1387 W. The electricity consumption of the rotary fan and automation system remained unchanged across the entire range of outside temperatures, amounting to 460 W. The heating capacity supplied to the room ranges from 4180 W to 5735 W. The uncertainty of the electrical power measurement is practically negligible, as it is equal to ±0.45%. The calculated expanded uncertainty of heating capacity, determined in accordance with the Guide to Uncertainty in Measurement (GUM) methodology [17], amounts to ±8.9% at a coverage factor of $k = 2$, corresponding to a confidence level of approximately 95%.

Heating capacity exhibited an increasing trend with decreasing outdoor air temperature. This phenomenon is a consequence of the decreasing temperature difference between the indoor and outdoor air as the outdoor temperature rises, which, at a constant mass flow rate and under maintained constant condensation pressure, results in a reduced heat flux delivered to the conditioned space. The electrical power consumption exhibits a slight decreasing trend with the increasing outdoor air temperature, driven by the gradual improvement in evaporator operating conditions: as the outdoor temperature rises, the evaporation temperature increases, reducing the pressure differential between the suction and discharge sides of the compressor, and thereby lowering the specific compression work.

Figure 14 shows the heating capacity of the device and its electrical power consumption at different outdoor temperatures.

Since both the heating capacity and the electrical power consumption decrease with increasing outdoor temperature at comparable rates, their ratio (COP) remains relatively stable across the investigated temperature range as shown in Fig 15. However, given the limited number of measurement series available, no statistically robust trend in COP as a function of outdoor temperature can be established from the present dataset, and this relationship warrants further investigation over a wider range of operating conditions. The COP of the heat pump with a ceramic regenerator was on average 3.70, and it reached the maximum value of 4.31 for the outside temperature of 1.1°C.

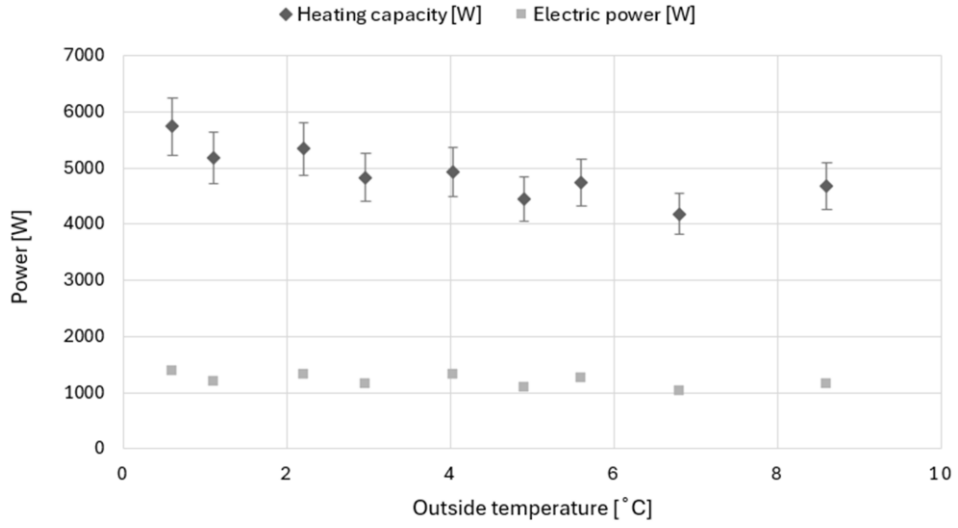


Fig. 14. Heating capacity and electric power vs. outside temperature.

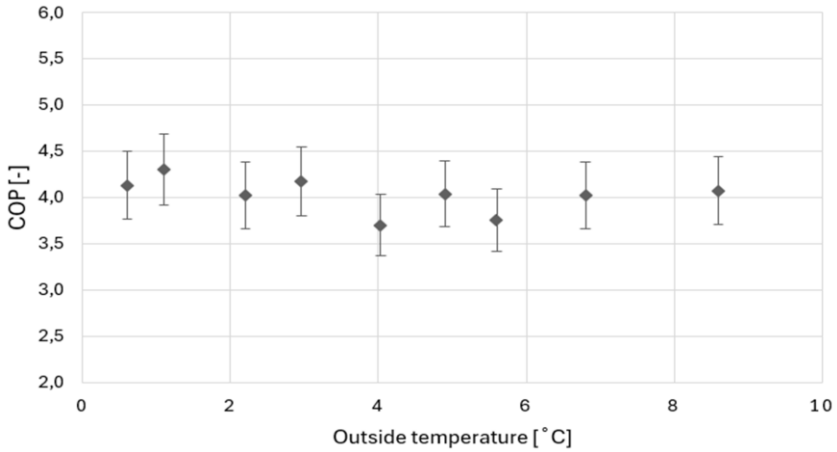


Fig. 15. COP vs. outside temperature.

4. Conclusions

This study experimentally characterised the performance of a compact reversible ventilation unit integrating a ceramic fixed-bed regenerator with an R290 vapour-compression heat pump. The following conclusions can be drawn from this study:

- Integration with an R290 vapour-compression heat pump enabled operation under the tested winter conditions without an auxiliary heat source. COP values of 3.70−4.31 were achieved at outdoor temperatures ranging from 0.6°C to 8.6°C, substantially exceeding 2.0−2.5 of conventional air-to-air heat pumps. The favourable evaporator conditions provided by warm exhaust air (~20°C) directly account for this elevated performance.
- Electrical power demand ranged from 1039 W to 1387 W, with the fan and automation contributing a constant 460 W. The average heating capacity ranged from 4180 to 5735 W, with characteristic double-capacity peaks during the supply phase from simultaneous regenerator and heat pump heat release.
- No water vapour condensation was observed in the ceramic matrix under any of the tested conditions, indicating that no electric pre-heating or defrosting was required during the experiments.
- The expanded COP uncertainty of ±8.9% (k = 2) is dominated by airflow (IRIS 250, ±5%) and humidity (SHT20, ±3% *RH*) measurements. Upgrading to a class 1 flowmeter and a ±1.5% *RH* sensor would reduce this to ~±4%. Future work should extend on testing below 0°C and investigating variable compressor speed effects on COP.

Acknowledgements

This study was conducted within the framework of a 501230104217 project conducted at the Institute of Heat Engineering of the Warsaw University of Technology and funded by Respireco sp. z o.o.

References

[1] Ministry of Infrastructure. (2022). *Regulation of the Minister of Infrastructure of 12 April 2002 on technical conditions to be met by buildings and their location* (consolidated text). Dz.U. 2022 item 1225 (in Polish)

[2] Rucinski, A., Grzebielec, A., Jaworski, M., Laskowski, R., Barylka, A., & Rusowicz, A. (2021). The problem of smog-particle removal in large cities – Experimental analysis of some filtration materials. *Energies*, 14(23), 8012. doi: 10.3390/en14238012

[3] Schumann, L., Hoerold, K.S., Tomaschewski, R.O., Cetin, Y.E., & Kriegel, M. (2026). Influence of a local ventilation system on patient and personnel protection in operating rooms. *Journal of Hazardous Materials*, 501, 140712. doi: 10.1016/j.jhazmat.2025.140712

[4] Dodoo, A., Gustavsson, L., & Sathre, R. (2011). Primary energy implications of ventilation heat recovery in residential buildings. *Energy and Buildings*, 43(7), 1566–1572. doi: 10.1016/j.enbuild.2011.02.019

[5] Niemierska, E., & Jadwiszczak, P. (2023). Experimental investigation of a ceramic heat regenerator for heat recovery in a decentralized reversible ventilation system. *International Communications in Heat and Mass Transfer*, 146, 106899. doi: 10.1016/j.icheatmasstransfer.2023.106899

[6] Aktershev, S.P., Mezentsev, I.V., & Mezentseva, N.N. (2022). Parametric study of a regenerative heat exchanger for ventilation with a periodic change in the air flow direction. *Applied Thermal Engineering*, 202, 117831. doi: 10.1016/j.applthermaleng.2021.117831

[7] Jedlikowski, A., Kanaś, P., & Anisimov, S. (2020). Heat and mass transfer inside the rotary heat exchanger operating under high speed rotor conditions. *International Journal of Heat and Mass Transfer*, 152, 119558. doi: 10.1016/j.ijheatmasstransfer.2020.119558

[8] Ventia Sp. z o.o. *Product catalog* [accessed 19 Feb. 2026]

[9] Kilkovský, B. (2020). Review of design and modeling of regenerative heat exchangers. *Energies*, 13(3), 759. doi: 10.3390/en13030759

[10] Liu, Z., Li, W., Chen, Y., Luo, Y., & Zhang, L. (2019). Review of energy conservation technologies for fresh air supply in zero energy buildings. *Applied Thermal Engineering*, 148, 544–566. doi: 10.1016/j.applthermaleng.2018.11.085

[11] Mikola, A., & Kõiv, T.-A. (2014). The efficiency analysis of the exhaust air heat pump system. *Engineering*, 6(13), 1037–1045. doi: 10.4236/eng.2014.613093

[12] Bani Issa, A.A., Liang, C., Groll, E.A., & Ziviani, D. (2025). Residential heat pump and air conditioning systems with propane (R290) refrigerant: Technology review and future perspectives. *Applied Thermal Engineering*, 266, 125560. doi: 10.1016/j.applthermaleng.2025.125560

[13] EN 378-1:2017-03. (2017). *Refrigerating systems and heat pumps—Safety and environmental requirements – Part 1: Basic requirements, definitions, classification and selection criteria*. European Committee for Standardization.

[14] International Electrotechnical Commission. (2022). *IEC 60539-1:2022 Directly heated negative temperature coefficient thermistors – Part 1: Generic specification*. Geneva, Switzerland.

[15] EN 308:2022. (2022). *Heat exchangers – Test procedures for establishing the performance of air-to-air heat recovery components*. Brussels, Belgium: European Committee for Standardization.

[16] Zawada, B. (2006). *Control systems in ventilation and air-conditioning systems*. Oficyna Wydawnicza Politechniki Warszawskiej (in Polish).

[17] Joint Committee for Guides in Metrology. (2008). *Evaluation of measurement data – Guide to the expression of uncertainty in measurement* (JCGM 100:2008). BIPM.

[18] Grzebielec, A. (2022). Investigation of a heat recuperator using ceramic inserts in winter and summer periods. *Szkło i Ceramika*, 2, 30–33 (in Polish).

[19] PN-EN 13141-8:2014-09. (2014). *Ventilation for buildings – Testing of performance of components/products for residential ventilation – Part 8: Performance testing of unducted mechanical supply and exhaust ventilation units (including heat recovery) for mechanical ventilation systems*. Polski Komitet Normalizacyjny, Warszawa, Poland (in Polish).